

## 5 Sensitivity to wind forcing

### 5.1 Introduction

Following the results of previous chapter, i.e. the used high-resolution model was under-predicting  $H_s$  and  $T_p$ , and wave models inaccuracies are historically attributed to the input winds, the model was run again using different wind fields. The obtained output was compared against the observations described in Chapter 2 to identify the main sources of error in the calculations along the fetch. The main purpose of the work presented in this chapter was to identify the contribution of the wind input to the under-predictions of the wave model.

First, it is important to understand how the wave model is dealing with the wind data being input in the form of WS and WiD. The source terms  $S_i$  in Equation 4-1 and Equation 3-5 were roughly presented in the previous chapter. The source terms related to the work described further on are  $S_{in}$  and  $S_{ds}$ , which represent the generation processes through wind input, and the dissipation processes through whitecapping, bottom friction and deep-induced braking. For clarity reasons, Equation 3-1 is reproduced again here:

$$S_{tot} = S_{in} + S_{nl} + S_{ds}$$

**Equation 5-1**

Wave generation is generally represented through two mechanisms describing the transfer of energy and momentum from the wind to the waves: Phillips (1957) considered that turbulent pressure fluctuations force free surface waves, resulting in a linear wave growth with time; Miles (1957) considered that resonant interactions between the wave induced air pressure fluctuation and the free surface waves resulted in a exponential growth of the waves. The general equation describing wave growth by wind is:

$$S_{in}(\sigma, \theta) = A + B \cdot E(\sigma, \theta)$$

**Equation 5-2**

In which  $A$  describes Phillip's linear growth and  $B$  Miles's exponential growth. The initial growth is described by the linear growth, but it is fast dominated by the exponential growth.  $E$  refers to the energy spectrum.

In SWAN, the linear growth is parameterized using Cavaleri and Malanotte-Rizzoli (1981) linear growth term (Ris 1997), and can be turned on or off to the user's will. The exponential growth has been parameterized by different authors in different forms. SWAN default formulation corresponds to an early version of WAM Cycle 3 due to Komen et al. (1994) (KOM). This expression is a function of  $U_*/c$ : the friction wind velocity ( $U_*$ ) and the phase velocity of the waves  $c$ .  $U_*$  is calculated using the drag coefficient  $C_D$  which, in this case, is only a function of  $WS$ .

The second available formulation for the exponential growth term as used in WAM Cycle 4 is due to Janssen (1989) and Janssen (1991), hereafter referred to as JAN. It is based on the quasi-linear wind-wave theory, which is dependent on the sea state through the calculation of  $U_*$ . In this case,  $C_D$  is a function of the roughness length, and thus, the sea state.

There is a third formulation described in Yan (1987), for which the wind-induced wave growth depends quadratically on  $U_*/c$  for strong wind conditions, and linearly for weaker wind forcing.

Wave energy dissipation through whitecapping is strongly related to the wind input formulation used. Therefore, the whitecapping formulation used with the first two wind input formulations (KOM and JAN) is described in Komen et al. (1984), and is characterized by a steepness dependent coefficient. Although it is the same whitecapping formulation, the (tunable) coefficients are different because they were obtained by closing a different energy balance equation in idealized wave growth conditions (different for each wind input formulation).

Yan (1987) wind input formulation is used with an adapted form of Alves and Banner (2003) whitecapping expression, based on its apparent relationship with wave groups, as described by van der Westhuysen, A. J. et al. (2007).

More details can be found on SWAN technical documentation manual (The SWAN team 2008).

## **5.2 Methodology**

To assess the adequacy of the wind fields, the wave model was run with the different wind fields described in Table 5-1. The first run (Run 1) was the reference run used in previous Chapter 4. In the present chapter, SWAN wave model was run using the default KOM formulation for wind input and whitecapping, except in the last run. The remaining SWAN settings are the same ones described in previous chapter.

**Table 5-1. Description of the wind fields used to run the SWAN wave model at 0.01° spatial resolution and 1h output temporal resolution.**

Run n°	Wind source	Spatial Distribution	Temporal resolution	Wave model settings
Run 1	MM5	Variable	3h	KOM
Run 2	2.1 A-dw(D)	Homogeneous	1h	KOM
	2.2 EMA-T	Homogeneous	1h	KOM
	2.3 EMA-U	Homogeneous	1h	KOM
Run 3	Max WS	Homogeneous	1h (interpolated)	KOM
Run 4	4.1 $\alpha$ *MM5 ( $\alpha = 1.1$ )	Variable	3h	KOM
Run 5	MM5	Variable	3h	JAN

SWAN was first run using the observed data at the three meteorological stations (Run 2) described in Chapter 2. It was assumed that the observations were the best winds available: WS and WiD recorded at each station were imposed to the whole domain in three different runs (2.1, 2.2 and 2.3). The resulting wind fields were homogeneous in space and non-stationary in time; the wind fields were input to the wave model every hour.

Within the land-ocean boundary layer where the transect was located, WS was expected to increase from the coast towards offshore; therefore, the model was expected to under-predict the observed  $H_s$  when using the coastal data, and to over-predict it when using the wind data from the offshore buoy A-dw(D). Flamant et al. (2003) reported increasing WS as a function of the distance from the coastline up to 50km offshore in the Gulf of Lions (north of the study region), which was linked to the acceleration of the flow associated to the different roughness of the land/sea transition. However,  $H_s$  was under-predicted in all three scenarios, as explained in next section. Also, because WS fields in the region were highly variable in space, in Run 3 the wave model was forced using the maximum WS predicted by the MM5 within a 0.1° wide strip along the instrumental transect (Figure 5-1).

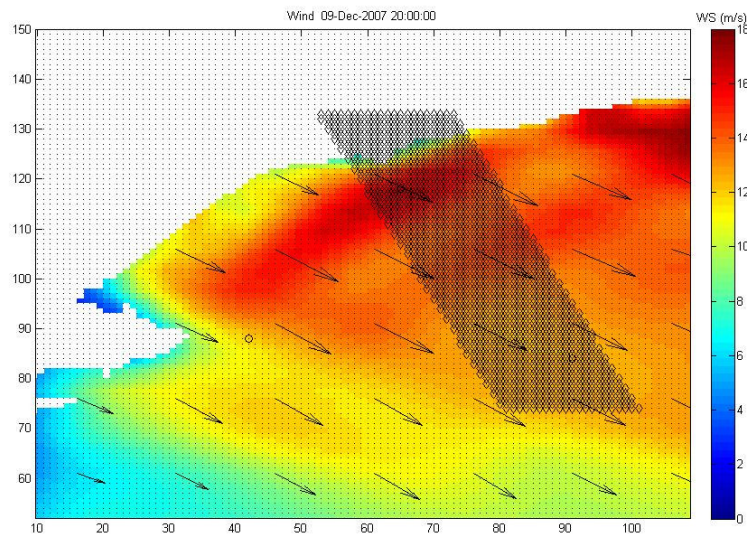


**Figure 5-1.** Wind fields predicted using 4km MM5 model in the region of study. The color scale indicates the values of WS. The arrows indicate the direction of the winds but are not scaled with WS. The shadowed region indicates the region from which the maximum WS was taken in Run 3.

Also, WS fields were calibrated to improve  $H_s$  predictions according to the work undertaken by Cavaleri and Bertotti (1997). They corrected  $H_s$  under-predictions increasing the WS in an enclosed basin using an enhancement factor  $\alpha = 1.5$ . They emphasized that  $\alpha$  may change depending on the characteristics of the basin and the resolution of the forcing model. Accordingly, in this work different enhancement factors were used (from 1.1 to 1.5) aiming to calibrate the MM5 WS in the region and to improve  $H_s$  predictions (Run 4).

Last, in Run 5 the JAN formulations for wind input and whitecapping explained in the previous section were used. The wave model was then run using the predicted MM5 winds used in Run 1.

The performance assessment mainly used the observations at A-dw(D) because predictions at this location were better than at the other buoys, as shown in previous chapter. The performance assessment at the other locations should be carried on in future work. The statistical analysis used agreed with the methodology presented in Chapter 3. The statistical estimators used were bias, RMSE, RMAE, MAE, SI and percentage of error.

### **5.3 Results**

Wind fields obtained from high resolution MM5 atmospheric model under-predicted  $H_s$  (Chapter 4). The observations at the meteorological stations were assumed to be the measure of wind available, and were used as input to SWAN. As expected, and according to Flamant et al. (2003), that reported WS increases from the coast towards offshore, the wind fields from the observations

at the coastal stations largely under-predicted  $H_s$  (-75% error) (Figure 5-2; Table 5-2). However, and unexpectedly, when using the winds at the offshore buoy A-dw(D) (Run 2.1),  $H_s$  at all the instruments was again under-predicted (on the order of 1m and up to 1.5m (-42% error) at A-dw(D)) (Figure 5-2; Table 5-2). Predicted  $H_s$  values were even smaller than the ones obtained using MM5 winds (Run 1; -17% error). According to MM5 predicted wind fields, the reason could be that the WS measured at A-dw(D) were not the highest WS across the fetch. Against what was expected from previous observations (Flamant et al. 2003) WS fields were here highly variable within the land-ocean boundary (Figure 5-1). This is easily understood considering the complex orography along the Catalan coast.

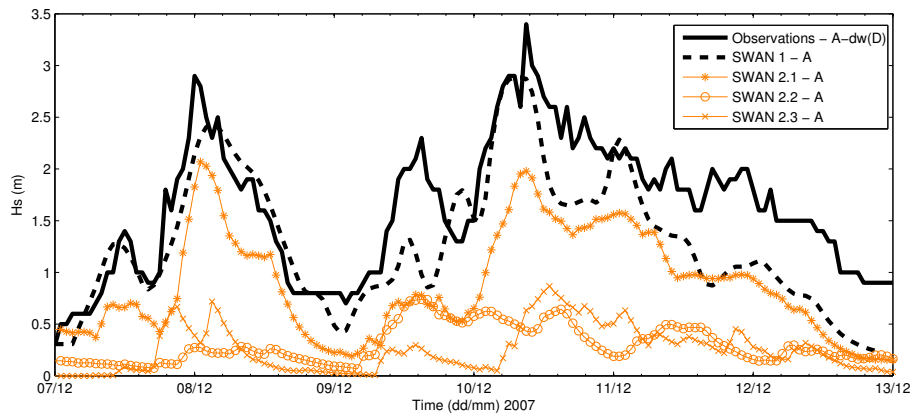


**Figure 5-2. Observed  $H_s$  and predicted  $H_s$  from SWAN runs 1 and 2.1 to 2.3, as described in Table 5-1, at the offshore buoy A-dw(D).**

The most representative results from the statistical analysis are summarized in Table 5-2 in terms of the percentage of error of the complete time series ( $T_p$ ) and at the storm peak ( $H_s$ ).  $H_s$  bias was only calculated at the peak of the storm because it is at this point that the consequences of the mis-predictions are more important. Also, as seen in previous chapters the statistical parameters of the whole series can be misleading.

**Table 5-2. Results from the different SWAN runs described in Table 5-1. Percentage of error between each model run and the observations at A-dw(D).**

Run n°		$T_p$	$H_s$ at the 2 <sup>nd</sup> storm peak
<b>Run 1</b>		- 26%	- 17%
<b>Run 2</b>	2.1	- 38%	- 42%
	2.2	- 59%	- 78%
	2.3	- 68%	- 75%
<b>Run 3</b>		- 15%	+ 1%
<b>Run 4</b>		- 22%	- 2%
<b>Run 5</b>		- 18%	+ 75%

Consequently, in Run 3 the wave model was run again using the maximum WS predicted along A-dw(D) fetch, expecting a large over-prediction of  $H_s$ . The mean difference of the so called maximum WS and the WS at A-dw(D) was about 4.5m/s (60.5%). However, the wave output results showed that the magnitude of  $H_s$  at the peak of the storm was comparable to the observations (Figure 5-3; Table 5-2), and not over-predicted (+1% error).

The conclusion was that stronger winds than the observed ones improve  $H_s$  predictions because the under-prediction is partially overcome. This was previously reported by Cavaleri and Bertotti (1997), who used enhancement factors of up to  $\alpha = 1.5$  on the wind input to properly reproduce  $H_s$  observations in a minor basin. In Run 4, it was stated that the best enhancement factor for the region of study was  $\alpha = 1.1$ . The mean difference between the enhanced WS and the WS at A-dw(D) was about 2.5m/s (45%). When MM5 winds were enhanced using this factor, predicted  $H_s$  reached the same magnitude than the observations at the storm peak (+2% error) (Figure 5-3; Table 5-2).

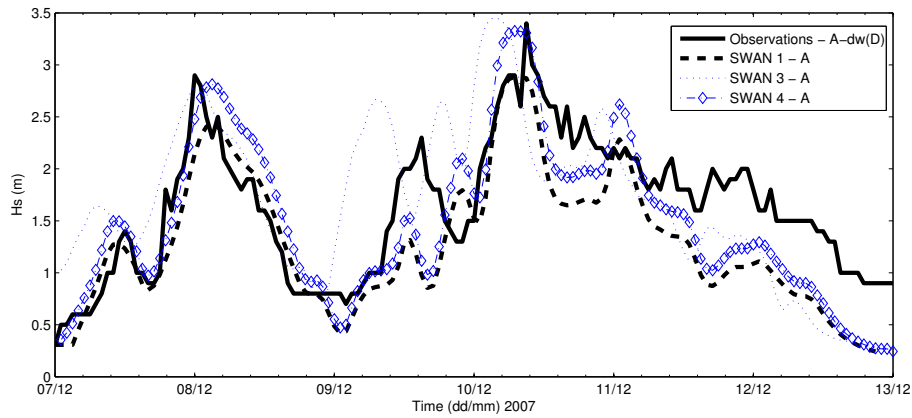


**Figure 5-3. Observed  $H_s$  and predicted  $H_s$  from SWAN runs 1, 3 and 4, as described in Table 1, at the offshore buoy A-dw(D).**

It was also observed that the best  $T_p$  predictions (-15% error) were obtained when using the maximum WS along the fetch (Run 3) (Figure 5-4; Table 5-2). The error between the predicted and the observed  $T_p$  was also smaller than when using the enhancement factor  $\alpha = 1.1$  (Run 4), for which only a slight improvement was observed (-22% error instead of -26% error in Run 1).

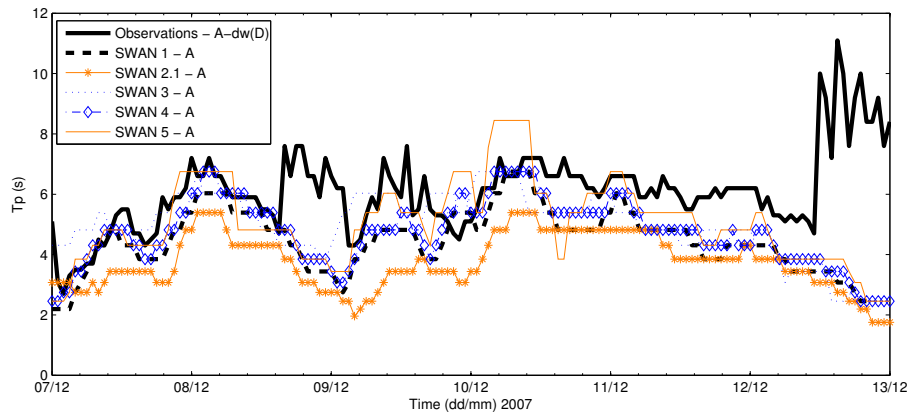


**Figure 5-4. Observed  $H_s$  and predicted  $H_s$  from the different SWAN runs described in Table 1, at the offshore buoy A-dw(D).**

The results up to that point indicated that to obtain accurate predictions an increase of WS was needed. However, the observational records indicated that WS was largely over-predicted. These

results suggest that the energy was inaccurately transmitted from the wind towards the waves: given the same amount of energy, generated waves should be higher, and energy should travel faster towards lower frequencies; i.e. observed  $H_s$  and  $T_p$  should increase faster than what was predicted. The drag coefficient  $C_D$  is the main link between the wind and the surface ocean waves. In KOM formulation,  $C_D$  is a function of WS only, whereas in JAN it is also a function of the energy spectrum or, in other words, the sea state. Therefore, JAN formulation seems more likely to enhance wave growth and thus, could improve SWAN wave predictions during the event of interest. In Run 5, SWAN was set to use the third-generation mode expressions due to JAN, but they lead to a large over-prediction of  $H_s$  (75%) (Figure 5-5; Table 5-2).  $T_p$  prediction was better than when using the KOM formulations and similar to the results obtained in Run 3 (Figure 5-4): the percentage of bias was -18%.

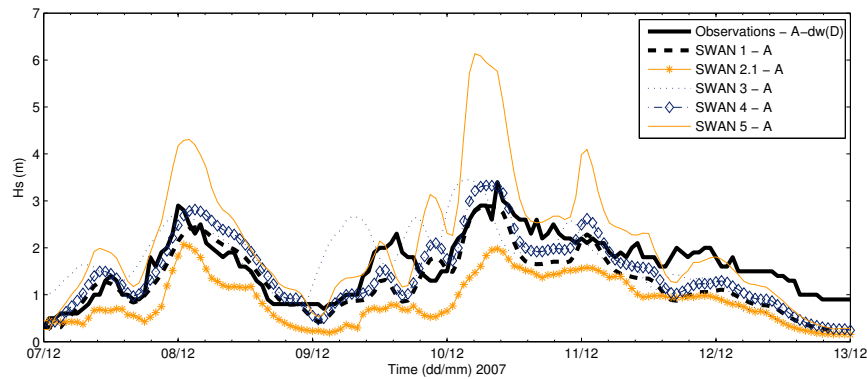


**Figure 5-5.** Observed  $H_s$  and predicted  $H_s$  from the different SWAN runs described in Table 1, at the offshore buoy A-dw(D).

Scatter plots in Figure 5-6 reproduce what was previously stated from the visual analysis. The bad performance of Run 3 ( $R^2 = 0.6$ ) was due to the fact that although the magnitude of  $H_s$  at the peak of the storm was properly reproduced, some peaks were mis-estimated (Figure 5-3).

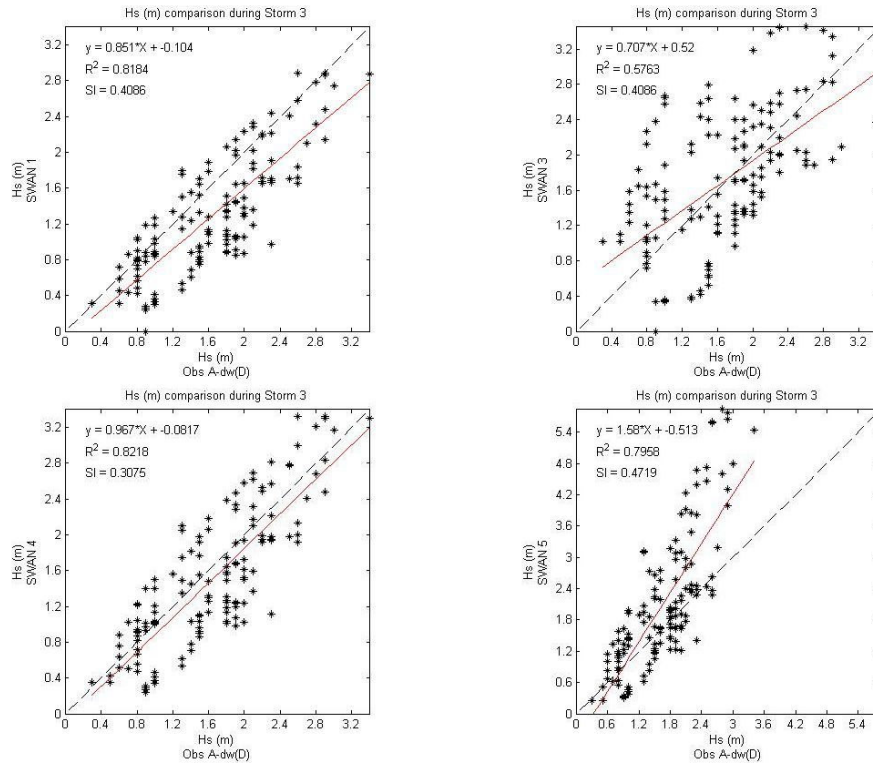


Figure 5-6.  $H_s$  scatter plots. A-dw(D) observations against SWAN different runs: Run 1 (up-left), Run 3 (up-right), Run 4 (down-left), and Run 5 (down-right). The red line is the linear equation that best fits the data points. The dashed line indicates the ideal fit (1:1 linear equation).

## 5.4 Discussion

To assess the importance of wind forcing in properly predicting the observed wave conditions, different wind fields were used and the importance of spatially variable over homogeneous wind fields was analyzed. The results indicated that using the maximum WS over the whole domain generated the same  $H_s$  at the storm peak than enhancing the spatially variable winds by a factor of 1.1. Using homogeneous winds,  $T_p$  increased faster with fetch and reached a better agreement with the observations at the different fetch lengths considered. The effect of changing WiD and the importance of spatial variability of the wind fields on wave growth should be further studied.

The use of enhancement factors was not aimed at improving the WS fields because the validation results already showed that the magnitude of the WS was over-predicted. The need of an enhancement factor pointed to an inaccurate transmission of energy from the wind towards the waves. The inaccuracy of predicted  $T_p$  and the evolution of the spectral shape with fetch indicated that the growth functions used were still not accurate at short fetches. In the future, these issues could be addressed by calibrating the dissipation coefficients of the used formulations, and/or by working on the drag coefficient ( $C_D$ ), which is the key mechanism of wind/wave interaction. Indeed, the formulations of wave models were calibrated according to theoretical wind-wave

growth curves that may differ significantly in highly variable regions like the southern Catalan coast.

The large over-prediction of  $H_s$  due to JAN formulation could be related to the convergence problems discussed in Niclasen (2006). Overall, it points to an implementation problem of JAN formulation in SWAN. Indeed, this set of expressions was specially formulated for WAM and it had historical problems in SWAN. One of the reasons, pointed out by Janssen in a personal communication, is the iterative procedure used in SWAN to solve the expression of  $U^*$ . WAM, instead, uses a table of values which makes the iteration much faster and robust. Niclasen (2006) argues that the convergence problem could be related to the Hersbach-Janssen limiter, which is used to guarantee numerical stability in SWAN (The SWAN team 2008). Also, preliminary results indicated that the observed over-prediction could only be related to the non-stationary mode of SWAN (and not to the stationary runs). In any case, these issues should be further studied and are included in Chapter 8 *Future work*.